Order of phase transitions and tricriticality in mixtures of octyloxycyanobiphenyl and nonyloxycyanobiphenyl liquid crystals: A high-resolution study by adiabatic scanning calorimetry

George Cordoyiannis,* Chandra Shekhar Pati Tripathi, Christ Glorieux, and Jan Thoen†
Laboratorium voor Akoestiek en Thermische Fysica, Departement Natuurkunde en Sterrenkunde, Katholieke Universiteit Leuven, Celestijnenlaan 200D, B-3001 Leuven, Belgium
(Received 2 July 2010; published 22 September 2010)

A detailed study has been performed for mixtures of octyloxycyanobiphenyl (8OCB) and nonyloxycyanobiphenyl (9OCB) liquid crystals and nine of their mixtures by means of high-resolution adiabatic scanning calorimetry. The isotropic to nematic transitions are weakly first order with latent heat values in the range usually encountered for this transition in other liquid crystals. With the exception of pure 8OCB, for which only an upper limit of 1.8 J kg^{-1} for the latent heat could be established, finite latent heats have been obtained for the nematic to smectic-*A* transition of all the mixtures and of pure 9OCB. The concentration dependence of their latent heats could be well fitted with a crossover function consistent with a mean-field free-energy expression that has a nonzero cubic term induced by the Halperin-Lubensky-Ma (HLM) coupling between the smectic-*A* order parameter and the orientational director fluctuations. Clearly first-order transitions with measurable latent heats are found for mole fractions of 9OCB in the mixtures where the effective critical exponent for the specific-heat capacity has substantially lower values than the tricritical one (0.5). This is qualitatively different from what has been observed so far in other liquid-crystal systems and yields strong experimental evidence from a calorimetric experiment for the HLM coupling between the smectic-*A* order parameter and the director orientation fluctuations.

DOI: 10.1103/PhysRevE.82.031707 PACS number(s): 42.70.Df, 65.40.Ba, 07.20.Fw, 64.70.M−

I. INTRODUCTION

Liquid-crystalline compounds can exhibit one or more mesophases with symmetry intermediate between that of an isotropic liquid and a solid crystal. These mesophases possess orientational order but no or reduced positional order [1–3]. Many different types of phase transitions occurring in liquid crystals have been good model systems for testing the general concepts of phase transitions and critical phenomena. The first-order (i.e., discontinuous) or second-order (i.e., continuous) character of the transitions and the universality class of the critical exponents have been investigated extensively by many different techniques.

The most frequently observed transition is the one between the isotropic (*I*) liquid phase and the nematic (*N*) phase, possessing only orientational order but no positional order. This transition is weakly first order [1–3] with small latent heats and quite often substantial pretransitional fluctuation effects [4]. However, the nematic to smectic-*A* (*N*-Sm*A*) phase transition is probably the most extensively studied and, at the same time, the most controversial in the field of liquid crystals [5]. In addition to the orientational order, the Sm*A* phase exhibits one-dimensional positional order. The positional order in the Sm*A* phase can be described in terms of a two-component complex order parameter and, thus, in general terms the *N*-Sm*A* transition should belong to the three-dimensional *XY* universality class (including, e.g., the normal to superconductor transition and the λ transition in helium [2]). However, the first molecular models that appeared almost 40 years ago resulted in a more complex picture [6,7]. It was predicted that the transition should be first order for $T_{NA}/T_{IN}>0.87$ and second order for $T_{NA}/T_{IN}<0.87$, where T_{NA} and T_{IN} are the isotropic to nematic (*I*-*N*) and the nematic to smectic-*A* (*N*-Sm*A*) transition temperatures, respectively. Hence, a tricritical point (TCP) should occur at $T_{NA}/T_{IN}=0.87$. Shortly after the development of the molecular models, a formulation using a Landau free-energy expansion including coupling between the (orientational) nematic order parameter (*S*) and the (amplitude of the) smectic-*A* order parameter was developed by de Gennes [8,9]. It was shown that a strong coupling (narrow nematic range) results in a first-order *N*-Sm*A* transition, while a weak coupling (wide nematic range) gives a second-order transition. Subsequently, Halperin, Lubensky, and Ma (HLM) predicted, in analogy with type-I superconductors [10] that, because of the coupling between the Sm*A* order parameter and the nematic director fluctuations, the *N*-Sm*A* transition should be always fluctuation-induced weakly first order [11]. The discontinuity was expected to be weak and decrease with decreasing the T_{NA}/T_{IN} ratio, but never vanish. Later on, a continuous behavior similar to type-II superconductors was also considered [12,13], predicting a three-dimensional *XY* behavior with inverted specific-heat-capacity amplitudes. Further theoretical progress considered the anisotropy in the critical behavior of the correlation lengths parallel and perpendicular to the smectic layers, induced by the finite splay stiffness [14–21]. This anisotropy has been treated by gauge transformation theory [14,17], dislocation-loop melting theory [15,16], and self-consistent one-loop theory [20,21].

In principle the above theoretical predictions apply to pure one-component liquid-crystalline systems or by extension to mixtures of liquid-crystalline compounds (usually of

*george.cordoyiannis@ijs.si
†Corresponding author; jan.thoen@fys.kuleuven.be

the same homologous series) in the one-component approximation. Other special situations such as the chirality of the compound (N^*-Sm*A* transition) [22,23] or the presence of nonmesogenic impurities [24,25] can affect the order of the transition and the pretransitional behavior. These special situations will not be further considered since here results are presented for octyloxycyanobiphenyl (8OCB) and nonyloxycyanobiphenyl (9OCB), two nonchiral compounds of the alkyloxycyanobiphenyl (nOCB) homologous series, and for some of their mixtures.

The many different types of phase transitions in liquid crystals have been studied extensively by a large variety of experimental techniques in efforts to determine the order of the phase transitions and the universality classes of the related critical phenomena. The work to be presented here concerns the *I*-*N* transition and the *N*-Sm*A* transition. Regarding the *I*-*N* transition the weakly first-order character is well established [4]. The values of the (effective) critical exponents describing the anomalies in relevant physical quantities are consistent with the presence of a (nearby) tricritical point [26–28]. The situation concerning the *N*-Sm*A* transition is still not clearly established and theoretically not fully understood. From many high-resolution calorimetric and x-ray studies it follows that the critical exponents α (specific-heat capacity), γ (susceptibility), and $\nu_{\|}$ and $\nu_{\perp}$ (parallel and perpendicular correlation lengths) exhibit complicated but systematic trends as functions of the McMillan ratio T_{NA}/T_{IN} [5]. For wide nematic ranges when α has the three-dimensional *XY* value, not all other critical exponents have three-dimensional *XY* values [5,29]. In particular, there remains a persistent critical anisotropy in the correlation length behavior. For T_{NA}/T_{IN} values very close to 1 the *N*-Sm*A* transition is clearly first order with latent heats (L) often comparable to the ones measured for the *I*-*N* transitions [30,31]. With decreasing T_{NA}/T_{IN} values (i.e., increasing the width of the nematic range) the latent heat values strongly decrease, becoming effectively zero (calorimetrically) at an apparent tricritical point in a quadratic way as a function of the mole fraction deviation from the tricritical value [32–34]. For even smaller T_{NA}/T_{IN} values the transitions are effectively second order and exhibit critical behavior with a specific-heat critical exponent α decreasing from the tricritical value $\alpha_{TCP}=0.5$ (at the tricritical point) to the three-dimensional *XY* value $\alpha_{3D-XY}=-0.007$ [32–36]. At first sight this picture is in full agreement with the crossover from second order to first order induced by increased de Gennes coupling between the smectic density-wave amplitude and the magnitude of the nematic order parameter [8,9]. However, it seems that the picture is more complicated. In 1987 Anisimov *et al.* [37] pointed out that there is an important difference between the Landau-de Gennes theory that does not include a cubic term (contrary to the HLM theory) and the experimental *N*-Sm*A* tricritical behavior. According to the Landau-de Gennes theory the latent heat should go to zero at the TCP as a function of the concentration difference in a linear way and not quadratically as observed experimentally. In Ref. [37] it was found that the discrepancy could be resolved by assuming a small cubic term in the Landau-de Gennes free-energy expansion. This was the first experimental evidence considered to be in line with the predictions of the HLM theory. In a 1990 paper by Anisimov *et al.* [38] a more extended experimental test for a HLM fluctuation-induced first-order character was presented. A universal scaling curve was used to reanalyze and compare previous results of the latent heat, obtained by high-resolution adiabatic scanning calorimetry (ASC), for 9CB+10CB (nonylcyanobiphenyl and decylcyanobiphenyl) [32], 8CB+10CB (octylcyanobiphenyl and decylcyanobiphenyl) [33], and (4-*n*-hexyloxy-phenyl-4′-*n* decyloxybenzoate and 4-*n*-hexyloxy-phenyl-4′-*n* dodecyloxybenzoate) [34] mixtures. A good description of the experimental data could be obtained. From an extrapolation of the curve fitting the measured latent heats (along the first-order part of the coexistence line), it was concluded that the experimental upper limits for the latent heats of transitions considered second order were larger than the estimated HLM contribution. Of particular relevance is the case of pure 8CB with an estimated HLM contribution substantially smaller than the upper limit $L=1.4$ J kg^{-1} quoted by Thoen *et al.* [39]. An analysis by Anisimov *et al.* [38] in terms of their scaling relation of previously published [40] *N*-Sm*A* interface front propagation velocity measurements yielded qualitative and quantitative evidence for the presence of HLM latent heat contribution consistent with the estimates from the calorimetric L data. In 1995 Tamblyn *et al.* [41] reported measurements of the capillary length near the apparent tricritical point of 8CB-10CB and obtained results consistent with the HLM analysis of Anisimov *et al.* [38]. More recently, Yethiraj *et al.* [42–46] introduced a novel intensity fluctuation microscopic technique for testing a fluctuation-induced first-order phase transition. Measurements were carried out for 8CB and some mixtures of 8CB and 10CB. From these measurements values of the entropy discontinuity were derived for pure 8CB and for four 8CB+10CB mixtures (see Fig. 2 of Ref. [44]). At concentrations above the (apparent) tricritical one (narrow *N* ranges), a good agreement was obtained with the direct calorimetric latent heats [33] and with the HLM scaling curve of [38]. However, for a lower 10CB concentration (i.e., wider *N* range) and especially for pure 8CB quite large latent heats are obtained. For 8CB they found a value more than an order of magnitude larger than the upper limit of Thoen *et al.* [39] and the HLM value of Anisimov *et al.* [38]. In addition, the effect of an external magnetic field was probed by the same technique, and it was found to be much weaker than predicted by HLM. In 2001 Lelidis [47] reported for 8CB a birefringence-derived discontinuity in the nematic order parameter at the *N*-Sm*A* transition corresponding to an enthalpy discontinuity (latent heat) about ten times larger than the calorimetry result and the HLM result [38,39,46]. At present, the origin of these inconsistencies is not understood. According to Herbut *et al.* [48] the inclusion of smectic fluctuations in the HLM calculation could possibly solve (part of) the discrepancies.

In view of the above uncertainties and discrepancies in the experimental situation new high-resolution experiments are clearly desirable. Since most of the relevant experiments have been carried out for compounds of the alkylcyanobiphenyl homologous series and mainly on the 8CB compound, we decided to look for suitable compounds for a high-resolution ASC investigation of the different but related

homologous series of the nOCBs. Two suitable compounds of this series are 8OCB and 9OCB. This series might exhibit a different strength of the HLM coupling between the Sm*A* order parameter and the nematic director orientation fluctuations. Investigations of 8OCB using the ac calorimetric technique did not show any evidence for a first-order coexistence region at the *N*-Sm*A* transition [49–55]. Using ASC Jamée *et al.* [23] did not find any evidence for a first-order character of the transition. An upper limit of $L=1.8$ mJ g^{-1} for a possible latent heat and a maximum width of a possible two-phase region of 2 mK were reported. Evidence for the first-order character of the *N*-Sm*A* transition of 9OCB was only recently presented on the basis of an investigation by means of modulated differential scanning calorimetry (MDSC) [56,57]. The phase diagram of the system 8OCB+9OCB was also qualitatively characterized and a tricritical point was reported for a $x=0.63$ mole fraction of 9OCB [56]. Additional MDSC data for the pure 8OCB were published in another paper by Sied *et al.* [58].

The paper is organized as follows. Section II gives some relevant theoretical background information. Section III describes the experimental setup and the measured samples. Section IV A discusses the results for the pure 8OCB and 9OCB. Mixture results are analyzed and discussed in Sec. IV B. A summary and conclusions are formulated in Sec. V.

II. THEORETICAL BACKGROUND

In the vicinity of the *I*-*N* transition the thermodynamic behavior is usually described with the Landau-de Gennes mean-field theory. For a uniaxial nematic liquid crystal one writes the free energy F as an expansion of the order parameter S,

$$F = F_o + \frac{1}{2}A_o S^2 - \frac{1}{3}B_o S^3 + \frac{1}{4}C_o S^4 + \frac{1}{6}E_o S^6. \tag{1}$$

In the isotropic phase $S=0$ and $F=F_o$, and in the nematic phase $S\neq 0$. In Eq. (1) one has $B_o>0$ and $A_o=a_o(T-T^*)/T_{IN}$, with $a_o>0$. T^* is the stability limit of the isotropic phase. The presence of the cubic term leads to a first-order transition at T_{IN} with a finite discontinuity, $S_{IN}=2B_o/3C_o$, in the order parameter. The excess heat capacity in the nematic phase is given by [1,2]

$$C_p = \frac{a_o^2}{C_o T_{IN}}\left[1 + \frac{B_o}{2(a_o C_o)^{1/2}}\left(\frac{T^{**}-T}{T_{IN}}\right)^{-1/2}\right], \tag{2}$$

with T^{**} being the stability limit of the nematic phase. At the *I*-*N* transition temperature T_{IN} there is a jump in C_p equal to $\Delta C_p = 2a_o^2/C_o T_{IN}$. For the enthalpy discontinuity (latent heat L) at T_{IN}, one obtains

$$\Delta H_L = H_I - H_N = \frac{2a_o B_o^2}{9C_o^2}. \tag{3}$$

Thus, because of the presence of the (small) cubic term in Eq. (1), the *I*-*N* transition is predicted to be (weakly) first order.

As pointed out in the introduction, the basic features of the initial molecular models of Kobayashi [6] and McMillan [7] for the *N*-Sm*A* transition can also be obtained from a Landau-de Gennes [8,9] free-energy expansion in terms of the smectic order parameter with the inclusion of coupling terms between the nematic and smectic order parameters. In this case, the smectic free energy $F_{NA}=F-F_N$ (with F_N as the nematic free energy) near the *N*-Sm*A* transition can be written as

$$F_{NA} = \frac{1}{2}a_o^*(T)|\Psi|^2 + \frac{1}{4}c_o|\Psi|^4 + \frac{1}{6}e_o|\Psi|^6 - d_o|\Psi|^2\delta S + \frac{1}{2\chi}\delta S. \tag{4}$$

For $T<T_{NA}$, one has $\delta S = S - S_o$, with $S_o(T)$ being the nematic order parameter in the absence of smectic order. The temperature dependence of a_o^* is given by $a_o^*(T)=\alpha_o(T-T_o)$. χ is the temperature-dependent nematic susceptibility that is large near T_{IN}, but decreases with decreasing temperature. The quantities α_o, c_o, e_o, d_o, and χ are all positive constants. On minimizing F with respect to δS, one gets $\delta S = C\chi\Psi^2$; and then eliminating δS from F yields

$$F_{NA} = \frac{1}{2}a_o^*(T)|\Psi|^2 + \frac{1}{4}c|\Psi|^4 + \frac{1}{6}e_o|\Psi|^6, \tag{5}$$

with $c=c_o-2d_o^2\chi$. Depending on the values of d_o and χ and the resulting sign of c, three different cases occur. For $c>0$ one has a continuous transition with $T_o=T_{NA}$, $c<0$ corresponds to first-order transitions, and at $c=0$ one has the crossover from second-order transitions to first-order transitions at the tricritical point.

In 1974 Halperin *et al.* [10,11] considered, in addition to the S-Ψ coupling, the contribution to F_{NA} of the δn-Ψ coupling also between the nematic director orientation fluctuations and the smectic order parameter. It was derived that a cubic term in Ψ always occurs in F_{NA}, making the transition (weakly) first order. The free energy can be written in the form [38]

$$F_{NA} = \frac{1}{2}A(T)|\Psi|^2 - \frac{1}{3}B|\Psi|^3 + \frac{1}{4}C|\Psi|^4 + \frac{1}{6}E|\Psi|^6. \tag{6}$$

In this equation $A=a'(T-T_o)/T_o$ (with $T_o\neq T_{NA}$), and $B,E>0$. At a Landau tricritical point (LTP), e.g., at a mole fraction x^* in a binary mixture of two liquid crystals, one has $C=0$. Assuming near the LTP along the T_{NA} phase-transition line $C=C'(x-x^*)$, with $C'<0$ and x as the mole fraction of the mixture, it is easy to show [38] that the entropy discontinuity at x^* can be written as

$$\Delta S^* = \frac{1}{2}a'\left(\frac{B}{2E}\right)^{2/3}. \tag{7}$$

It can also be shown that close to the LTP the reduced entropy difference $s\equiv\Delta S/R$ (with R as the gas constant) at mole fraction x is related to $s^*\equiv\Delta S^*/R$ at x^* in the following way:

$$\left(\frac{s}{s^*}\right) - \left(\frac{s}{s^*}\right)^{-1/2} = \frac{\hat{a}}{s^*}(x - x^*) = y - y^*, \tag{8}$$

with $\hat{a} = -3\alpha'/8E$. Introducing the new variables $y \equiv \hat{a}x/s^*$ and $y^* \equiv \hat{a}x^*/s^*$, a universal function for s/s^* of the distance to the LTP can be constructed.

III. EXPERIMENTAL SETUP AND SAMPLES

For the measurements reported in this paper we have used ASC. Adiabatic scanning calorimetry was developed to obtain simultaneously and continuously the evolution of the heat capacity C_p and the enthalpy H as a function of temperature [59]. Both quantities can be studied with very high precision and temperature resolution, while maintaining a thermal equilibrium within the sample. In order to obtain $C_p(T)$ and $H(T)$, a constant power P is supplied to the sample and the resulting change in temperature $T(t)$ is measured as a function of time t. From P and $T(t)$, the heat capacity can easily be calculated as follows:

$$C_p = \frac{P}{\dot{T}(t)}, \tag{9}$$

with $\dot{T}(t) = dT/dt$ as the time derivative of the temperature to be calculated by numerical differentiation of $T(t)$. However, the exact knowledge of $T(t)$ allows also the direct calculation of the enthalpy H as a function of temperature by inverting the $T(t)$ data to

$$H(T) = H(T_s) + P[t(T) - t_s(T_s)], \tag{10}$$

with T_s as the temperature of the run starting at t_s. The continuous and precise assignment of the enthalpy as a function of temperature provides a unique tool for the determination of the order of a phase transition. When the enthalpy shows a jump at a certain temperature (i.e., a latent heat is present), the transition is first order; when such a jump is absent the transition is second order (or continuous). In the case of a broadened first-order transition the two-phase region can clearly be identified. The ASC measurements have been performed with a computer-controlled calorimeter consisting of three stages. The sample cell that could contain up to 3 g of sample was made of tantalum and equipped with a resistive heating wire and a thermistor as a temperature sensor. Inside the cell there was also a stirring ball. Stirring in the horizontally mounted cylindrical cell was achieved by periodically changing the inclination of the plate supporting the calorimeter, allowing the stirring ball to roll back and forth in the cell. Further details on the ASC method and the practical implementations can be found elsewhere [31,59,60].

The liquid crystals 8OCB and 9OCB were purchased from BDH. Both compounds were carefully stored prior to the measurements, and they were used as received. A sample of the same 8OCB batch was measured in a similar calorimeter by Jamée *et al.* [23]. This measurement was repeated as an additional check of the quality of the sample, and it yielded sharp transitions and the same transition temperatures with only a few mK difference. Several mixtures of 8OCB and 9OCB were also prepared, namely, $x = 0.85$, 0.75, 0.70, 0.66, 0.62, 0.59, 0.50, 0.30, and 0.15. The concentration x is defined as the molar ratio of 9OCB in the mixture $n_{9OCB}/(n_{9OCB}+n_{8OCB})$, i.e., pure 9OCB and 8OCB correspond to the values of 1 and 0, respectively. Prior to the measurements, all mixtures were kept for several hours in the I phase and stirred in order to ensure homogeneous mixing. Afterward, cooling runs (with rates of ~ 0.1 K h^{-1}) were performed in the range including the I-N and N-SmA transitions. Additional very slow heating runs (with rates of ~ 0.03 K h^{-1}) were performed in the vicinity of the N-SmA transition in order to provide data for precise critical fits.

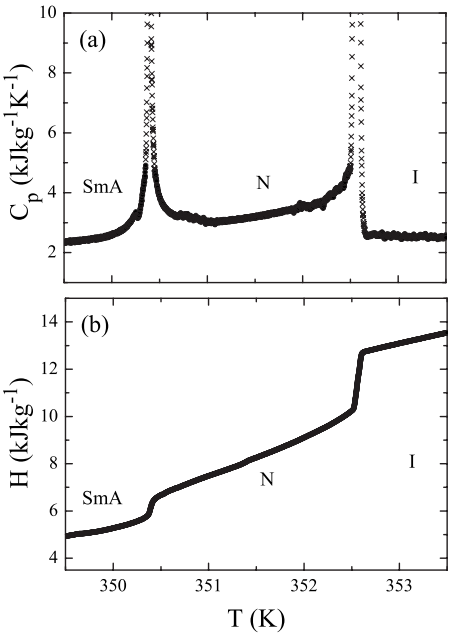

FIG. 1. (a) Temperature dependence of the specific-heat capacity of 9OCB from well in the smectic-A phase to well in the isotropic phase (solid dots). The crosses correspond to the effective values in the two-phase regions. (b) Temperature dependence of the enthalpy over the corresponding range. For display reasons a linear temperature-dependent background $2.1(T - T_{ref})$ (kJ kg^{-1}), with T_{ref} an arbitrary reference temperature, has been subtracted.

IV. RESULTS AND DISCUSSION

For the pure 8OCB compound calorimetric data obtained by ac calorimetry [49–55], ASC [23], and MDSC [56–58] have been reported. The pure compound 9OCB has only been investigated by MDSC [56,57]. For three mixtures of 8OCB and 9OCB additional MDSC results have been published [56]. Here, we give a full account of different ASC results for the two pure compounds 8OCB and 9OCB and for nine of their mixtures [61].

A. Pure compounds 8OCB and 9OCB

1. Overview of the results

In Figs. 1(a) and 1(b) an overview is given for the experimental heat capacity $C_p(T)$ and the enthalpy $H(T)$ over a temperature range from well in the SmA phase to well in the isotropic phase for the pure 9OCB compound. The I-N and

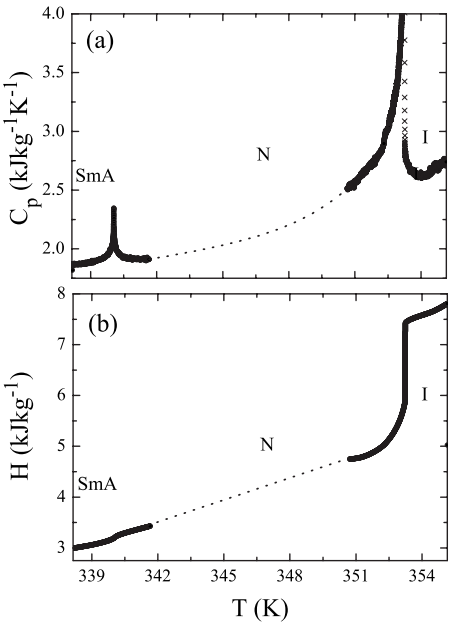

FIG. 2. (a) Temperature dependence of the specific-heat capacity of 8OCB in the Sm*A* and *N* phases around the *N*-Sm*A* transition and in the *N* and *I* phases around the *I*-*N* transition (solid symbols). The crosses correspond to the effective values in the two-phase region. (b) Temperature dependence of the enthalpy over the corresponding range. For display reasons a linear temperature-dependent background $2.1(T-T_{ref})$ (kJ kg^{-1}), with T_{ref} as an arbitrary reference temperature, has been subtracted. The dotted lines serve only as guides to the eye.

N-Sm*A* transitions are clearly visible in both quantities. In Figs. 2(a) and 2(b) a similar overview is presented for the pure 8OCB. One may notice the substantial difference between the width of the nematic range of 9OCB (about 2.2 K) and that of 8OCB (about 13 K). Because high-resolution ASC measurements have only been done near both phase transitions for 8OCB and not in the large intermediate nematic range, both data sets in Fig. 2 have been connected by dotted lines to guide the eye. From the enthalpy plots of Figs. 1(b) and 2(b) it is clear that in both cases the *I*-*N* transitions are discontinuous, which is consistent with Eq. (3). For 8OCB we obtain for the latent heat $L=1.55\pm0.05$ kJ kg^{-1} and for 9OCB $L=2.4\pm0.1$ kJ kg^{-1}. These *I*-*N* latent heats as well as the pretransitional heat-capacity behavior below and above the transition are similar and in line with the behavior of other systems [4], and they will not be further considered. We will concentrate on the *N*-Sm*A* transitions of 8OCB and 9OCB and of their mixtures, where quantitative and qualitative differences are encountered. From the enthalpy curves in Figs. 1(b) and 2(b) it is not obvious whether or not there is an enthalpy discontinuity at the *N*-Sm*A* transitions within the resolution of these figures. One has to analyze the data near the *N*-Sm*A* transitions in more detail. In particular, this involves in the first place enlarging of small part of the enthalpy curves around the transitions and subtracting the often quite large regular (linear) increase in the enthalpy with temperature (corresponding to a constant background heat capacity). In these detailed plots one then looks for slope discontinuities at the beginning and end temperatures of the two-phase regions of first-order transitions. Looking at higher temperature derivatives of $H(T)$ is often quite helpful in determining the width of the two-phase region. From the enthalpy change over the two-phase region the latent heat can be determined. When the transition is second order, there is no two-phase region and no latent heat, but from the finite resolution of the $H(T)$ data a maximum width of a possible two-phase region and an upper limit for the possible latent heat can be assessed.

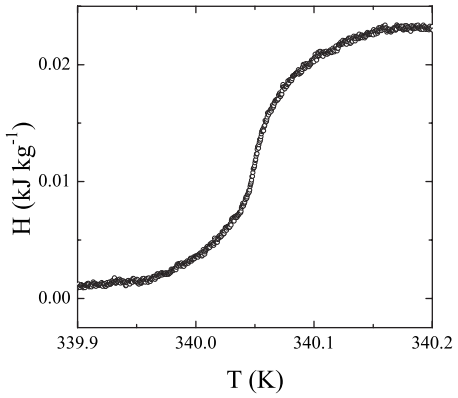

FIG. 3. Temperature dependence of the enthalpy near the *N*-Sm*A* phase transition of 8OCB over a 300 mK temperature range. For display reasons a linear temperature-dependent background $2.1(T-T_{ref})$ (kJ kg^{-1}), with T_{ref} as an arbitrary reference temperature, has been subtracted.

2. N-SmA phase transition in 8OCB

In Fig. 3 the temperature dependence of the enthalpy near the *N*-Sm*A* transition of 8OCB is given in a narrow temperature range of 300 mK. For display reasons a linear temperature-dependent background has been subtracted from the enthalpy. There is no clear indication of a latent heat at this transition. From a detailed analysis of the $H(T)$ and corresponding $C_p(T)$ data very near the transition we arrived at an upper limit of a latent of 1.8 J kg^{-1}. This is in agreement with the upper limit of 1.8 J kg^{-1} reported by Jamée *et al.* [23]. The data near the transition are consistent with a latent heat of 0.9 ± 0.9 J kg^{-1} and a two-phase region of about 2 mK. However, a zero latent heat and the second-order nature of the transition cannot be excluded. There is a substantial pretransitional heat-capacity variation on both sides of the transition temperature, which can be described by power-law expressions. The limiting behavior of the specific-heat capacity at a second-order transition can be described by means of a power law of the form

$$C_p = A^{\pm}|\tau|^{-\alpha} + B, \tag{11}$$

with $\tau=(T-T_c)/T_c$, $A^{\pm}$ as the critical amplitudes above (+) and below (−) the transition, α as the critical exponent, T_c as the critical temperature, and B as the constant background contribution composed of a regular and a critical contribution: $B=B_{reg}+B_c$. In a constant power heating or cooling run one readily arrives at the heat capacity C_p in Eq. (9) from the (known) power and from the temperature-dependent rate, by a numerical differentiation of $T(t)$ (the precisely and fre-

quently measured temperature evolution of the sample as a function of time). However, the fact that via Eq. (10) $T(t)$ can immediately be transformed in an enthalpy versus temperature curve opens new possibilities for the data analysis. At the temperature T with a corresponding enthalpy $H(T)$, two quantities with the dimensions (J kg^{-1} K^{-1}) of specific-heat capacity, C_p and C, can be introduced. C_p corresponds to the slope dH/dT of the enthalpy curve at T, and C is defined as

$$C = \frac{H - H_c}{T - T_c}, \tag{12}$$

and it corresponds to the slope of the chord connecting $H(T)$ at T and H_c at T_c. It can easily be shown that C has also a power-law behavior, but with an amplitude divided by $(1-\alpha)$ [39]. Thus, both C_p and C have the same critical exponents and background term, but different amplitudes. By considering the difference $(C-C_p)$, above and below T_c, the (unimportant) background term drops out, resulting (after taking the logarithm) in

$$\log(C - C_p) = \log\left(\frac{\alpha A^{\pm}}{1-\alpha}\right) - \alpha \log|\tau|. \tag{13}$$

Thus, one obtains a straight line with a (negative) slope directly yielding the critical exponent α. Equations (11) and (13) should only be used for data fitting sufficiently close to T_c. For extended C_p data ranges one uses the usual renormalization-group form with the inclusion of corrections-to-scaling terms [5,62]

$$C_p = A^{\pm}|\tau|^{-\alpha}(1 + D^{\pm}|\tau|^{\Delta}) + B + E(T - T_c). \tag{14}$$

Here, the superscripts $\pm$ again stand for above and below T_c. $D^{\pm}$ are the corrections-to-scaling amplitudes and Δ is the first corrections-to-scaling exponent. The value of Δ is usually set to the three-dimensional XY value of 0.529 [63] or to the essentially equivalent value of 0.5. B is again the sum of the regular and the critical backgrounds. The last term represents the temperature dependence of the regular contribution. From the definition of the quantity C in Eq. (12) the corresponding extended expressions for C and $(C-C_p)$ can be derived [39]. For $(C-C_p)$ one obtains

$$C - C_p = \frac{\alpha A^{\pm}}{1-\alpha}|\tau|^{-\alpha}\left[1 + D^{\pm}\left(1 - \frac{\Delta}{\alpha(1+\Delta-\alpha)}\right)|\tau|^{\Delta}\right] - \frac{E}{2}(T - T_c). \tag{15}$$

The corrections-to-scaling amplitudes as well as the coefficient of the linear background term are modified compared to Eq. (14). The linear background amplitude has changed sign and it is divided by 2. The multiplicative factor $f = 1 - \Delta\alpha^{-1}(1+\Delta-\alpha)^{-1}$ depends mainly on the (effective) value of α (assuming a fixed value around 0.5 for Δ). One has, e.g., $f=-2.57$ for $\alpha=0.1$, $f=-0.39$ for $\alpha=0.3$, and $f=0$ for the tricritical value $\alpha_{TCP}=0.5$. For $\alpha_{3D-XY}=-0.01$ a value $f=34.1$ is obtained. For a N-SmA transition close to the I-N transition the C_p peak is superimposed on the nematic pretransitional C_p wing of the I-N transition, often resulting in a nonlinear temperature dependence of the regular background. For this reason it is a common practice in the analysis of the direct C_p data to subtract this regular temperature-dependent background from the data and fit the difference with Eq. (14), where the free parameter B represents only B_c and E is set to zero [50,51]. Since in Eq. (15) the B value at T_c is not present anymore only the temperature dependence of the regular background, represented by the last term in Eq. (15), has to be considered. In nonlinear least-squares fitting (neglecting possible higher-order background terms) of the $(C-C_p)$ data with Eq. (15), E can be a free parameter or given a fixed value derived from the C_p or C behavior in the SmA and the N phases away from the transition. From our 8OCB data we arrived at a value $E=12$ kJ kg^{-1} K^{-2}. In the analysis of the $(C-C_p)$ data for 8OCB we did not use Eq. (15) in a nonlinear least-squares approach. Instead we have used, for the data relatively close to T_c, range shrinking and linear fitting (of the data above and below T_c simultaneously) with Eq. (13), before and after subtracting a linear contribution $E(T-T_c)/2$, with $E=12$ kJ kg^{-1} K^{-2}. The results for the effective exponent α and for the amplitude ratio A^-/A^+ of these fits are summarized in Table I. The values for the effective exponent α are all in the range between 0.18 and 0.23, while the amplitude ratio values are in the range between 1.08 and 0.97. There are slight differences between the fits with $E=0$ and $E\neq 0$. In the former case an average value $\alpha=0.213\pm0.013$ and in the latter one a value $\alpha=0.193\pm0.012$ are obtained. For the fits with $E=0$ an average value 1.042 ± 0.040 (i.e., larger than 1) is found for the amplitude ratio, whereas for $E\neq 0$ the corresponding average value is 0.997 ± 0.015 (i.e., slightly smaller than 1). An overall average value of $\alpha=0.20\pm0.02$ is in very good agreement with the value $\alpha=0.18\pm0.02$ derived from the data of Jamée *et al.* [23,64]. Most of the α values obtained in ac calorimetric experiments fall also in the range $\alpha=0.20\pm0.05$ [50,51,59,60]. The older ac data of Johnson *et al.* [49] resulted in a logarithmic singularity. For one sample LeGrange and Mochel [52,53] reported a value α

TABLE I. Parameters from the fits of the quantity $(C-C_p)$ near the N-SmA phase transition of 8OCB without and with an additional linear background term $-E(T-T_c)/2$ over various reduced temperature ranges.

E (kJ kg^{-1} K^{-2})	$\log_{10}(\lvert\tau\rvert_{min})$	$\log_{10}(\lvert\tau\rvert_{max})$	α_{eff}	A^-/A^+
0	−4.50	−3.00	0.224	1.003
12	−4.50	−3.00	0.205	0.975
0	−4.50	−2.75	0.222	1.074
12	−4.50	−2.75	0.200	1.009
0	−4.75	−3.00	0.210	1.008
12	−4.75	−3.00	0.192	0.986
0	−4.75	−2.75	0.214	1.077
12	−4.75	−2.75	0.193	1.012
0	−5.00	−3.00	0.200	1.012
12	−5.00	−3.00	0.183	0.984
0	−5.00	−2.75	0.208	1.078
12	−5.00	−2.75	0.187	1.013

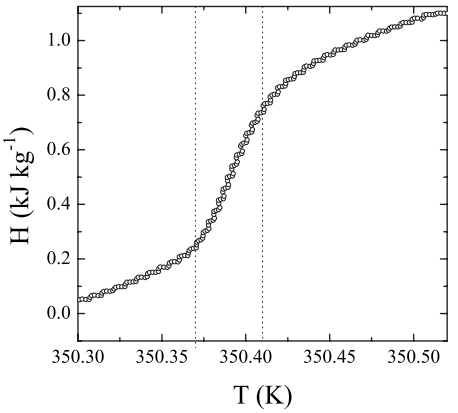

FIG. 4. Temperature dependence of the enthalpy near the *N*-Sm*A* phase transition of 9OCB over a 600 mK temperature range. For display reasons a linear temperature-dependent background $1.75(T-T_{ref})$ (kJ kg^{-1}), with T_{ref} as an arbitrary reference temperature, has been subtracted. The two vertical dotted lines represent the limits of the two-phase region.

$=0.025\pm0.04$, while another sample gave $\alpha=0.25\pm0.02$. Impurities were put forward as a possible cause for the low value. On the other hand, from their MDSC measurements Sied *et al.* [56] reported $\alpha=0.044\pm0.002$.

3. N-SmA phase transition in 9OCB

In Fig. 4 the temperature dependence of the enthalpy near the *N*-Sm*A* transition of 9OCB is given in a narrow temperature range of 600 mK. For display reasons a linear temperature-dependent background has been subtracted from the enthalpy. The transition is clearly first order. From a detailed analysis of the enthalpy $H(T)$ data and the corresponding specific-heat data $C_p(T)$ near the transition, we arrive at a two-phase region of 35 ± 2 mK and a latent heat $L=0.46\pm0.05$ kJ kg^{-1}. This value is about 30 times smaller than the latent heat of the *I*-*N* phase transition of this compound. From MDSC measurements Sied *et al.* [56] reported a value of 0.16 kJ/mol (i.e., 0.49 kJ kg^{-1}). From DSC measurements (at a scanning rate of 5 K min^{-1}) Oweimreen and Morsy [65] obtained a value of 1.2 kJ kg^{-1}. As can be seen in Fig. 1(a), on both sides of the *N*-Sm*A* transition, there is substantial pretransitional $C_p(T)$ change on approaching the transition. This temperature variation of $C_p(T)$ will be further considered in connection with mixtures also exhibiting a first-order *N*-Sm*A* transition.

B. Mixtures of 8OCB and 9OCB

In addition to the two pure compounds 8OCB and 9OCB, nine different mixtures of these compounds have been studied in detail near the *N*-Sm*A* transition by ASC. In Fig. 5 the *I*-*N* and the *N*-Sm*A* transition temperatures are plotted as functions of the mole fraction x of 9OCB. The T_{IN} values are consistent with a linear connection between the almost equal T_{IN} values of the two pure compounds. The T_{NA} transition line is slightly curved, and it can be fitted with a quadratic expression.

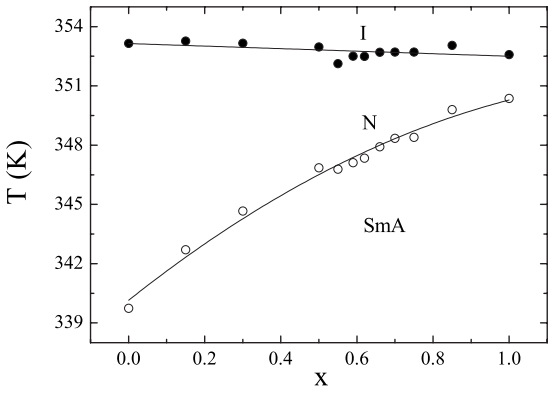

FIG. 5. Transition temperatures of 8OCB and 9OCB and of the different mixtures investigated, as a function of mole fraction x of 9OCB. Solid symbols are for the *I*-*N* transition and open symbols are for the *N*-Sm*A* transition. The solid line through the T_{IN} data is a linear fit. The solid line through the T_{NA} data is a quadratic fit.

1. Enthalpy behavior near the N-SmA phase transition

In Fig. 6 parts of the enthalpy curves of the pure 8OCB and of the three mixtures with the lowest 9OCB concentrations are given. In Fig. 7 a similar plot is presented for the other mixtures and for the pure 9OCB. For display reasons, because of the large differences in latent heat enthalpy changes, the results are presented in two separate figures. For the same reason also a linear temperature-dependent background has been subtracted from the enthalpy data. From a detailed inspection of $H(T)$ and $C_p(T)$ very near the *N*-Sm*A* transitions of the different mixtures the latent heat L values given in the lower part of Fig. 8 have been obtained. Both L and $L^{1/2}$ are plotted as functions of the mole fraction x of 9OCB. The mole fraction dependence is better visible in $L^{1/2}$ than in L at low latent heat values. It should also be noted that contrary to the 9CB+10CB and 8CB+10CB systems [32,33], $L^{1/2}$ here is not a linear function of the mole fraction.

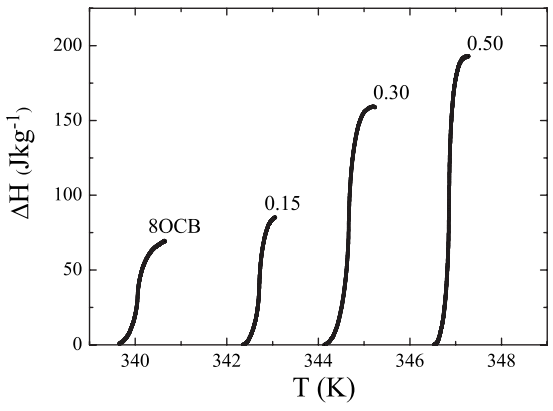

FIG. 6. Temperature dependence of the enthalpy near the *N*-Sm*A* phase transition of 8OCB and three mixtures of 8OCB +9OCB with 9OCB mole fractions of $x=0.15$, 0.30, and 0.50. For display reasons a linear temperature-dependent background $1.75(T-T_{ref})$ (kJ kg^{-1}), with T_{ref} as an arbitrary reference temperature, has been subtracted.

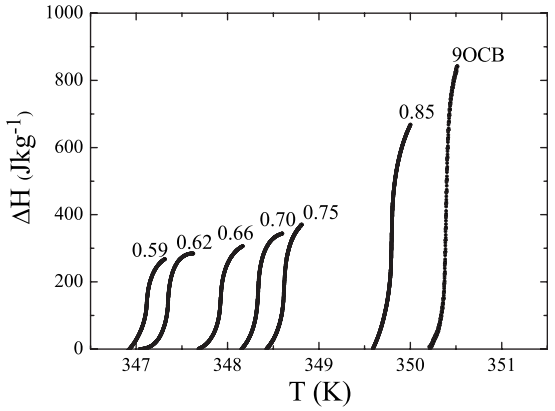

FIG. 7. Temperature dependence of the enthalpy near the *N*-Sm*A* phase transition of 9OCB and six mixtures of 8OCB +9OCB with 9OCB mole fractions of x=0.59, 0.62, 0.66, 0.70, 0.75, and 0.85. For display reasons a linear temperature-dependent background $1.75(T-T_{ref})$ (kJ kg^{-1}), with T_{ref} as an arbitrary reference temperature, has been subtracted.

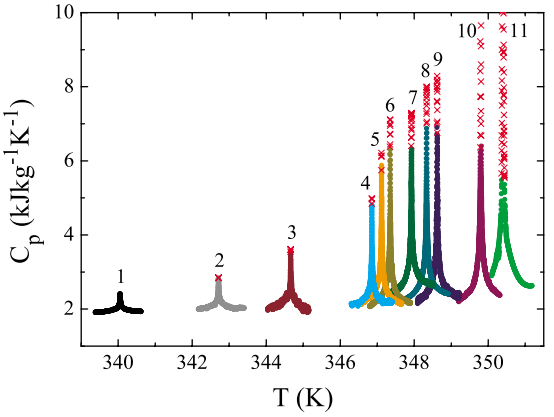

FIG. 9. (Color online) The specific-heat capacity C_p near the *N*-Sm*A* transitions at different mole fractions x of 9OCB in the mixtures and of pure 8OCB and 9OCB. From left to right data are displayed for increasing mole fraction x of 9OCB. 1: pure 8OCB; 2: x=0.15; 3: x=0.30; 4: x=0.50; 5: x=0.59; 6: x=0.62; 7: x=0.66; 8: x=0.70; 9: x=0.75; 10: x=0.85; 11: pure 9OCB. The crosses indicate the effective C_p values in two-phase regions of the first-order transitions.

2. *Specific-heat-capacity behavior near the N-SmA phase transition*

In Fig. 9 an overview is given of the temperature dependence of the specific-heat capacity C_p, as calculated with Eq. (9), in the immediate vicinity of the *N*-Sm*A* transitions for the nine mixtures as well as for the pure 8OCB and 9OCB. It should be noted that for the first-order transitions the calculated C_p values in the two-phase regions are effective ones. These two-phase region data can be distinguished from the real C_p values in the Sm*A* and *N* phases, and they are represented by different symbols (crosses). In Fig. 9 a clear increase in the C_p wings in the Sm*A* and *N* phases with increasing x can be observed, and there is also an increase in the values of the effective critical exponent α_{eff} for the mixtures with larger 9OCB mole fractions. This can indeed be seen in Fig. 10 where the results for separate fits with Eq. (13) (in the range $-4.25 \leq \log_{10}|\tau| \leq -3.0$ and with H_c and T_c adjustable parameters) for the smectic-*A* phase below the transition and in the nematic phase above the transition are given. The increased slopes of these lines indicate increased α_{eff} values. For display reasons the data for x=0.85 and 1.00 are not included in Fig. 10. However, all the obtained values for α_{eff} are displayed in the top part of Fig. 8. For the mixture x=0.85, α_{eff}=0.49 ± 0.03, and for the pure 9OCB α_{eff} =0.46 ± 0.04 is obtained. The pure 9OCB value is slightly smaller than the tricritical value of 0.5 and than the value α_{eff}=0.51 ± 0.03 of Cusmin *et al.* [57] from MDSC results. Contrary to the systems 8CB+10CB [33] and 9CB+10CB [32] the tricritical value α_{TPC}=0.5 is not obtained for a mixture where, within the experimental resolution, the latent heat is zero, but for a mixture near x_{9OCB} between 0.75 and 0.80 with a latent heat around 50 Jk g^{-1}.

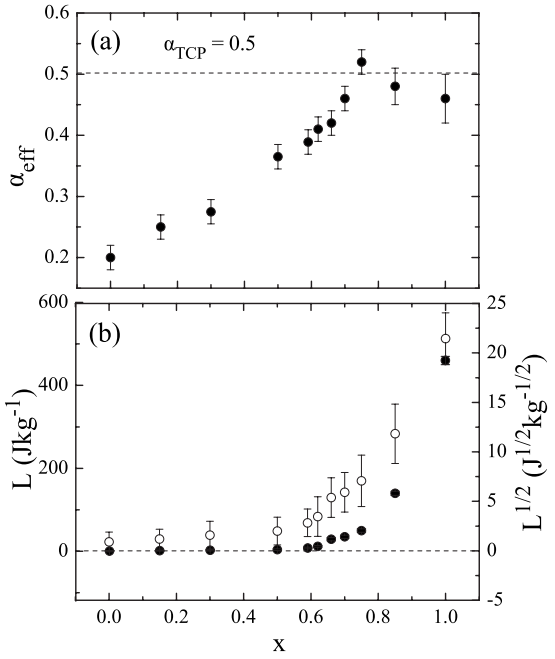

FIG. 8. (a) The effective critical exponent α_{eff} as a function of the mole fraction x of 9OCB. (b) The x dependence of the latent heat L (solid circles) and of the square root $L^{1/2}$ of the latent heat (open circles).

C. *N*-Sm*A* phase transition and evidence for a cubic term in the free energy

1. *Fit of the N-SmA latent heats of 8OCB+9OCB as a function of mole fraction*

As already pointed out in Sec. II, Halperin *et al.* [10] predicted that, because of the coupling between the nematic director orientation fluctuations and the smectic order parameter, a cubic term should always be present in the free-energy expansion, making the transition (weakly) first order. Anisimov *et al.* [34,38] on the basis of Eq. (6) arrived at the universal function of Eq. (8) for the reduced entropy discontinuity s near a LTP. They analyzed the data available at that time with Eq. (8). Here, a similar analysis of our new

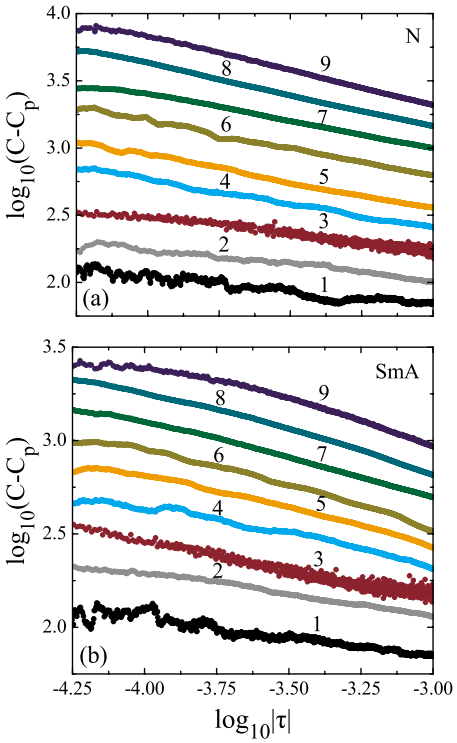

FIG. 10. (Color online) Double-logarithmic plots of the $(C-C_p)$ data as a function of $|\tau|$ (a) in the N phase and (b) in the SmA phase at different mole fractions x of 9OCB in the mixtures. From top to bottom data are displayed for increasing mole fraction x of 9OCB in the mixtures. 1: pure 8OCB, 2: $x=0.15$; 3: $x=0.30$; 4: $x=0.50$; 5: $x=0.59$; 6: $x=0.62$; 7: $x=0.66$; 8: $x=0.70$; 9: $x=0.75$.

8OCB+9OCB data is presented and, moreover, a comparison with the older data is made.

In Fig. 11 a fit with Eq. (8) of the reduced entropy discontinuity $s=\Delta S/R$ for the 8OCB+9OCB system is given as a function of the mole fraction of 9OCB for all the mixtures. A quite good fit is obtained. Since for 8OCB only an upper limit (of 1.8 J kg^{-1}) for a possible latent heat could be obtained experimentally, 8OCB was not included in the fit. The extrapolation of the fitting curve to $x=0$ resulted in an estimated latent heat for 8OCB of 0.85 J kg^{-1}, which is completely consistent with the 8OCB enthalpy data. From the fit a Landau tricritical point is obtained for a mixture with a mole fraction $x^*=0.8350$. The Eq. (8) fit parameters for this system are given in Table II. In that table we also give the parameter values from new fits of the old 9CB+10CB and 8CB+10CB [32,33,66] data and the parameter values for $\bar{6}O\overline{10}+\bar{6}O\overline{12}$ from Anisimov *et al.* [38].

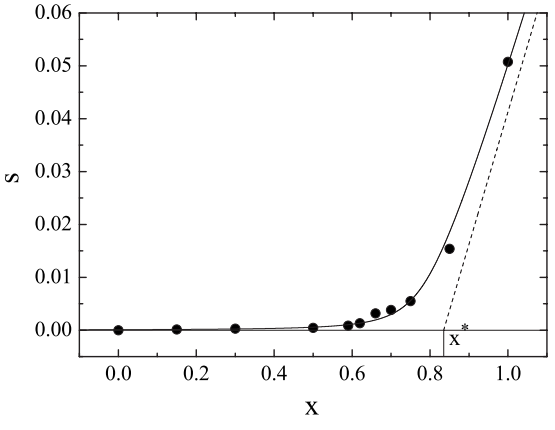

FIG. 11. The reduced entropy discontinuity $s=\Delta S/R$ (with R being the gas constant) for 8OCB+9OCB mixtures fitted to the scaling function of Eq. (8) to determine x^* of the Landau tricritical point and $s^*=\Delta S^*/R$. The data point for pure 8OCB was not included in the fit. The dashed line represents the Landau theory without the cubic term in Eq. (6).

TABLE II. Parameters values in Eq. (8) obtained from fitting the new data of 8OCB+9OCB, and the data of 9CB+10CB and 8CB+10BC from [32,33]. The values of $\bar{6}O\overline{10}+\bar{6}O\overline{12}$ are taken from Ref. [38].

Mixture	$\hat{a}$	x^*	s^*
8CB+10CB	0.9860	0.4213	0.02467
9CB+10CB	0.5917	0.0985	0.02029
8OCB+9OCB	0.2503	0.8350	0.01593
$\bar{6}O\overline{10}+\bar{6}O\overline{12}$	1.947	0.4828	0.0408

2. *Universal crossover relation and Landau tricritical point*

In Fig. 12 the reduced entropy discontinuities s/s^* are plotted as functions of $y-y^*$, as introduced in the universal crossover expression given in Eq. (8) for all the systems investigated accurately and in sufficient detail. From this figure it is quite clear that the new 8OCB+9OCB results are fully consistent with the data of the three older systems and follow the same crossover relation. This is more obvious for the low s/s^* in Fig. 13 where $\log_{10}(s/s^*)$ is plotted as a function of $y-y^*$. In that figure for 8CB and 8OCB, calorimetrically considered as second order within the experimental resolution, only the upper limits are indicated by vertical error bars. On the basis of an extrapolation of the fitting

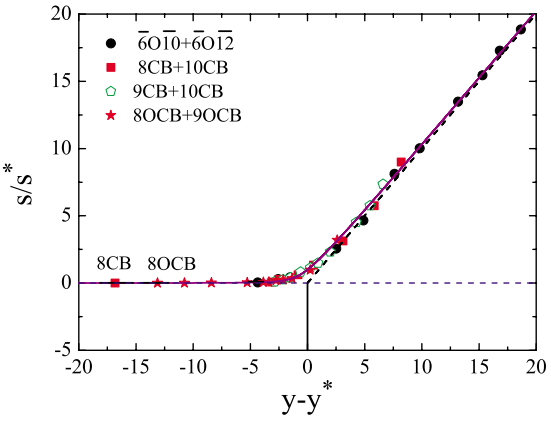

FIG. 12. (Color online) Normalized universal scaling representation of Eq. (8) for the four different kinds of mixtures considered. The solid line is based on the HLM mean-field free energy of Eq. (6). The heavy dashed line represents the Landau theory without the cubic term in Eq. (14).

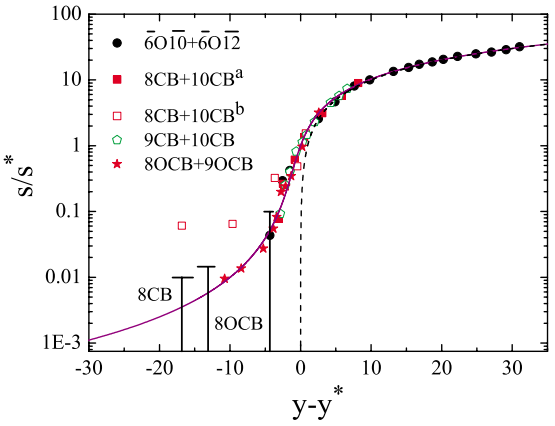

FIG. 13. (Color online) The normalized universal scaling representation of Fig. 12 with s/s^* on a logarithmic scale. Upper limits (and error bars) are shown for the data that have not been included in the fits. The data points for 8CB+10CB[a] are obtained from Ref. [33], and those for 8CB+10CB[b] are from Ref. [46]. The data for $\bar{6}O\bar{10}+\bar{6}O\bar{12}$ are from Ref. [38].

curve one would expect a latent heat roughly a factor of 2 smaller than the upper limits. As already mentioned in the introduction, Yethiraj *et al.* [42–46] derived from optical measurements of fluctuations in the nematic phase values for the entropy discontinuity at the *N*-Sm*A* transition of the pure 8CB and for four mixtures of 8CB+10CB. The corresponding s/s^* values are also displayed in Fig. 13. Three of the s/s^* values for $y-y^*$ values close to zero (near the Landau tricritical point) are consistent with the HLM curve, but the two other results (for pure 8CB and the 8CB+10CB mixture with a 10CB mole fraction of 0.18 in the mixture) are an order of magnitude larger than the corresponding values on the HLM curve and the calorimetric upper limit for 8CB. At present, it is not clear how these inconsistencies can be understood.

In Fig. 14 the mole fraction dependence of the effective critical exponent α_{eff} is compared with that of the latent heats for the system 8OCB+9OCB. In this figure it can be seen that α_{eff} reaches the tricritical value of 0.5 for a mole fraction of 9OCB closer to the mole fraction of the LTP (x

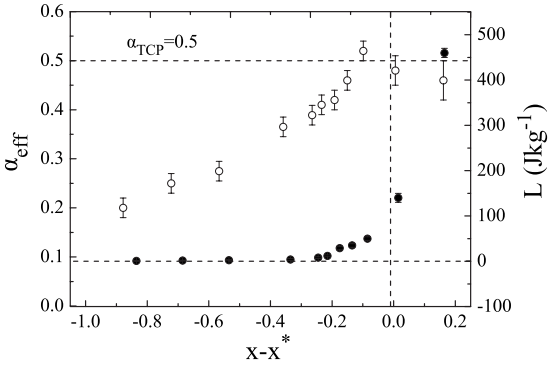

FIG. 14. Effective critical exponents α_{eff} (open circles) and latent heats L (closed circles) for mixtures of 8OCB+9OCB as functions of the mole fraction difference $(x-x^*)$ with the mole fraction x^* of the Landau tricritical point.

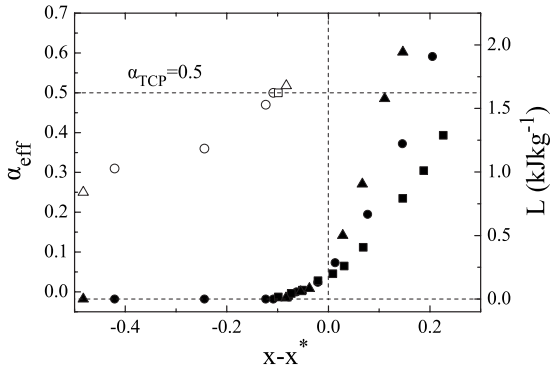

FIG. 15. Effective critical exponents α_{eff} and latent heats L for mixtures of 8CB+10CB (open and closed circles) from Ref. [33], 9CB+10CB (open and closed squares) from Refs. [32,33], and $\bar{6}O\bar{10}+\bar{6}O\bar{12}$ (open and closed triangles) from Refs. [34,38] as functions of the mole fraction difference $(x-x^*)$, with x^* as the mole fraction of the Landau tricritical point. For the 9CB+10CB and 8CB+10CB systems x is the mole fraction of 10CB in the mixture, while for $\bar{6}O\bar{10}+\bar{6}O\bar{12}$ it is the mole fraction of $\bar{6}O\bar{12}$.

$-x^*=0$) than for the previously studied systems presented in Fig. 15. It is also clear that finite latent heats are observed for α_{eff} values substantially smaller than $\alpha_{TCP}=0.5$. This is qualitatively different from what can be observed in the similar plot of Fig. 15, where for all three other systems α_{eff} reaches the value of $\alpha_{TCP}=0.5$ when the (possible) latent heat is smaller than the experimental limits. The difference in latent heat when $\alpha=0.5$ between the 8OCB+9OCB system and the other systems is presumably due to a larger cubic coefficient B in Eq. (6) for 8OCB+9OCB than for the other mixtures.

V. SUMMARY AND CONCLUSIONS

This paper reported on a detailed investigation by adiabatic scanning calorimetry of the liquid crystals octyloxycyanobiphenyl (8OCB) and nonyloxycyanobiphenyl (9OCB) and nine of their mixtures. Particular emphasis was given to the enthalpy and specific-heat capacity along the *N*-Sm*A* phase-transition line. All the *I*-*N* transitions were first order and exhibited latent values comparable with those observed in many other systems [4]. With the exception of the pure 8OCB, for all the mixtures and for the pure 9OCB finite latent heat values along the *N*-Sm*A* transition line have been found. For 8OCB only an upper limit for a possible latent heat L of 1.8 J kg^{-1} has been obtained. However, the enthalpy data are quite consistent with $L=0.9\pm0.9$ J kg^{-1}. The measured *N*-Sm*A* latent values could be well fitted with the crossover function of Eq. (8) consistent with a mean-field free-energy expression that has a cubic term [38]. The existence of such a cubic term implies that the *N*-Sm*A* transition is expected to be (weakly) first order. The existence of such a term was predicted in 1974 by Halperin *et al.* [10]. In this study we have found that clearly first-order *N*-Sm*A* transitions, with measurable latent heats, are obtained for mole fractions of 9OCB in the mixture where the effective critical exponents α_{eff} are as low as 0.25–0.30, which is substan-

tially lower than the tricritical value $\alpha_{TCP}=0.5$. This is qualitatively different from what was found in the three previously studied systems of 8CB+10CB, 9CB+10CB, and $\bar{6}O\bar{1}0+\bar{6}O\bar{1}2$. Moreover, in contrast to the previous results the mole fraction at which α_{eff} reaches $\alpha_{TCP}=0.5$ is very close to the mole fraction x^* of the Landau tricritical point, obtained by fitting the latent heat data with Eq. (8). These two specific features of the present calorimetric results for the 8OCB+9OCB system constitute strong evidence, resulting from a static experiment, for the HLM arguments for a cubic term in the free-energy expansion and the (weakly) first-order nature of the *N*-Sm*A* transition.

ACKNOWLEDGMENTS

This work was supported by the FWO (Project "AVISCO" No. G.0230.07) and the Research Fund of K. U. Leuven. The authors would like to thank C. W. Garland, P. H. Keyes, and T. C. Lubensky for stimulating discussions.

[1] G. Vertogen and W. H. de Jeu, *Thermotropic Liquid Crystals: Fundamentals* (Springer-Verlag, Berlin, 1988).
[2] P. G. de Gennes and J. Prost, *The Physics of Liquid Crystals* (Oxford University Press, Oxford, 1993).
[3] P. J. Collings and M. Hird, *Introduction to Liquid Crystals: Chemistry and Physics* (Taylor & Francis, London, 1997).
[4] B. Van Roie, J. Leys, K. Denolf, C. Glorieux, G. Pitsi, and J. Thoen, Phys. Rev. E **72**, 041702 (2005).
[5] C. W. Garland and G. Nounesis, Phys. Rev. E **49**, 2964 (1994), and references therein.
[6] K. Kobayashi, Phys. Lett. **31A**, 125 (1970).
[7] W. L. McMillan, Phys. Rev. A **4**, 1238 (1971).
[8] P. G. de Gennes, Solid State Commun. **10**, 753 (1972).
[9] P. G. de Gennes, Mol. Cryst. Liq. Cryst. **21**, 49 (1973).
[10] B. I. Halperin, T. C. Lubensky, and S. K. Ma, Phys. Rev. Lett. **32**, 292 (1974).
[11] B. I. Halperin and T. C. Lubensky, Solid State Commun. **14**, 997 (1974).
[12] C. Dasgupta and B. I. Halperin, Phys. Rev. Lett. **47**, 1556 (1981).
[13] J. Bartholomew, Phys. Rev. B **28**, 5378 (1983).
[14] T. C. Lubensky and J. H. Chen, Phys. Rev. B **17**, 366 (1978).
[15] D. R. Nelson and J. Toner, Phys. Rev. B **24**, 363 (1981).
[16] J. Toner, Phys. Rev. B **26**, 462 (1982).
[17] T. C. Lubensky, J. Chim. Phys. Phys.-Chim. Biol. **80**, 31 (1983).
[18] J. Prost, Adv. Phys. **33**, 1 (1984).
[19] C. Dasgupta, J. Phys. (Paris) **48**, 957 (1987).
[20] B. R. Patton and B. S. Andereck, Phys. Rev. Lett. **69**, 1556 (1992).
[21] B. S. Andereck and B. R. Patton, Phys. Rev. E **49**, 1393 (1994).
[22] C. W. Garland, Liq. Cryst. **26**, 669 (1999), and references therein.
[23] P. Jamée, G. Pitsi, and J. Thoen, Phys. Rev. E **67**, 031703 (2003).
[24] K. Denolf, B. Van Roie, C. Glorieux, and J. Thoen, Phys. Rev. Lett. **97**, 107801 (2006).
[25] K. Denolf, G. Cordoyiannis, C. Glorieux, and J. Thoen, Phys. Rev. E **76**, 051702 (2007), and references therein.
[26] P. H. Keyes, Phys. Lett. **67A**, 132 (1978).
[27] M. A. Anisimov, V. M. Zaprudskii, V. M. Mannetskii, and E. L. Sorkin, JETP Lett. **30**, 491 (1979).
[28] M. A. Anisimov, E. E. Gorodetskii, and V. M. Zaprudskii, Sov. Phys. Usp. **24**, 57 (1981).
[29] C. W. Garland, G. Nounesis, M. J. Young, and R. J. Birgeneau, Phys. Rev. E **47**, 1918 (1993), and references therein.
[30] J. Thoen, Int. J. Mod. Phys. B **9**, 2157 (1995).
[31] J. Thoen, G. Cordoyiannis, and C. Glorieux, Liq. Cryst. **36**, 669 (2009).
[32] J. Thoen, H. Marynissen, and W. Van Dael, Phys. Rev. Lett. **52**, 204 (1984), and references therein.
[33] H. Marynissen, J. Thoen, and W. Van Dael, Mol. Cryst. Liq. Cryst. **124**, 195 (1985).
[34] M. A. Anisimov, V. P. Voronov, A. O. Kulkov, V. N. Petukhov, and F. Kholmurodov, Mol. Cryst. Liq. Cryst. **150B**, 399 (1987).
[35] D. Brisbin, R. DeHoff, T. E. Lockhart, and D. L. Johnson, Phys. Rev. Lett. **43**, 1171 (1979).
[36] K. J. Stine and C. W. Garland, Phys. Rev. A **39**, 3148 (1989).
[37] M. A. Anisimov, V. P. Voronov, E. E. Gorodetskii, V. E. Podnek, and F. Kholmurodov, JETP Lett. **45**, 425 (1987).
[38] M. A. Anisimov, P. E. Cladis, E. E. Gorodetskii, D. A. Huse, V. E. Podneks, V. G. Taratuta, W. van Saarloos, and V. P. Voronov, Phys. Rev. A **41**, 6749 (1990).
[39] J. Thoen, H. Marynissen, and W. Van Dael, Phys. Rev. A **26**, 2886 (1982).
[40] P. E. Cladis, W. van Saarloos, D. A. Huse, J. S. Patel, J. W. Goodby, and P. L. Finn, Phys. Rev. Lett. **62**, 1764 (1989).
[41] N. Tamblyn, P. Oswald, A. Miele, and J. Bechhoefer, Phys. Rev. E **51**, 2223 (1995).
[42] A. Yethiraj and J. Bechhoefer, Mol. Cryst. Liq. Cryst. **304**, 301 (1997).
[43] R. Mukhopadhyay, A. Yethiraj, and J. Bechhoefer, Phys. Rev. Lett. **83**, 4796 (1999).
[44] A. Yethiraj and J. Bechhoefer, Phys. Rev. Lett. **84**, 3642 (2000).
[45] A. Yethiraj and J. Bechhoefer, Liq. Cryst. Today **10**, 1 (2001).
[46] A. Yethiraj, R. Mukhopadhyay, and J. Bechhoefer, Phys. Rev. E **65**, 021702 (2002).
[47] I. Lelidis, Phys. Rev. Lett. **86**, 1267 (2001).
[48] I. F. Herbut, A. Yethiraj, and J. Bechhoefer, EPL **55**, 317 (2001).
[49] D. L. Johnson, C. F. Hayes, R. J. deHoff, and C. A. Schantz, Phys. Rev. B **18**, 4902 (1978).
[50] C. W. Garland, G. B. Kasting, and K. J. Lushington, Phys. Rev. Lett. **43**, 1420 (1979).
[51] G. B. Kasting, K. J. Lushington, and C. W. Garland, Phys. Rev. B **22**, 321 (1980).
[52] J. D. LeGrange and J. M. Mochel, Phys. Rev. Lett. **45**, 35

(1980).
[53] J. D. LeGrange and J. M. Mochel, Phys. Rev. A **23**, 3215 (1981).
[54] I. Hatta and N. Nokoyama, Mol. Cryst. Liq. Cryst. **66**, 97 (1981).
[55] J. M. Viner and C. C. Huang, Solid State Commun. **39**, 789 (1981).
[56] M. B. Sied, J. Salud, D. O. López, M. Barrio, and J. L. Tamarit, Phys. Chem. Chem. Phys. **4**, 2587 (2002).
[57] P. Cusmin, M. R. de la Fuente, J. Salud, M. A. Pérez-Jubindo, S. Diez-Berart, and D. O. Lopéz, J. Phys. Chem. B **111**, 8974 (2007).
[58] M. B. Sied, D. O. López, J. L. Tamarit, and M. Barrio, Liq. Cryst. **29**, 57 (2002).
[59] J. Thoen, E. Bloemen, H. Marynissen, and W. Van Dael, *Proceedings of the 8th Symposium on Thermophysical Properties*, National Bureau of Standards, Maryland, 1981, edited by J. V. Sengers (American Society of Mechanical Engineers, New York, 1982), p. 422–428.
[60] J. Thoen, in *Heat Capacities: Liquids, Solutions and Vapours*, edited by E. Wilhelm and T. M. Letcher (The Royal Society of Chemistry, London, 2010), Chap. 13.
[61] A partial account of some of the 8OCB and 9OCB data as well as of preliminary data for a mixture of a 0.55 mole fraction of 9OCB has been given in Ref. [31]. The preliminary results of that run at $x_{9OCB}=0.55$ exhibited substantial rounding (considered second order in Ref. [31]), and they are not included in the final results here.
[62] F. J. Wegner, Phys. Rev. B **5**, 4529 (1972).
[63] R. Guida and J. Zinn-Zustin, J. Phys. A **31**, 8103 (1998).
[64] Unfortunately, the value of $\alpha=0.18\pm0.02$ was not explicitly cited in Ref. [23].
[65] G. A. Oweimreen and M. A. Morsy, Thermochim. Acta **346**, 37 (2000).
[66] The parameter values for 8CB+10CB and 9CB+10CB in Table II are slightly different from the ones reported in Ref. [38]. This is most likely resulting from the fact that we had access to the numerical values of the latent heat of these systems, while in Ref. [38] these values must have been deduced from the figures in Refs. [32,33].